



Archived at the Flinders Academic Commons:

<http://dspace.flinders.edu.au/dspace/>

This is the publisher's copyright version of this article.

The original can be found at:

<http://dx.doi.org/DOI: 10.1117/12.759260>

Jane, A., Szili, E., Reed, J.H., Gordon, T.P., & Voelcker, N.H., "Porous silicon biosensor for the detection of autoimmune diseases". Proceedings of SPIE, 6799, 679908-1-679908-11. (2007).

Copyright 2007 Society of Photo-Optical Instrumentation Engineers. One print or electronic copy may be made for personal use only. Systematic reproduction and distribution, duplication of any material in this paper for a fee or for commercial purposes, or modification of the content of the paper are prohibited.

Porous silicon biosensor for the detection of autoimmune diseases

Andrew O. Jane^{*a}, Endre J. Szili^a, Joanne H. Reed^b, Tom P. Gordon^b,
Nicolas H. Voelcker^a

^aFlinders University of South Australia, School of Chemistry, Physics and Earth Sciences,
GPO Box 2100, Bedford Park, South Australia, 5042, Australia

^bDepartment of Immunology, Allergy and Arthritis, Flinders Medical Centre,
GPO Box 2100, Bedford Park, South Australia, 5042, Australia

ABSTRACT

Advances in porous silicon (pSi) technology have led to the development of new sensitive biosensors. The unique optical properties of pSi renders the material a perfect candidate for optical transducers exploiting photoluminescence or white light interference effects. The ability of biosensors exploiting these transduction mechanisms to quickly and accurately detect biological target molecules affords an alternative to current bioassays such as enzyme-linked immunosorbent assays (ELISAs). Here, we present a pSi biosensor that was developed to detect antibodies against the autoimmune protein La. This protein is associated with autoimmune diseases including rheumatic disorders, systematic lupus erythematosus (SLE) and Sjogren's syndrome (SS). A fast and sensitive detection platform such as the one described here can be applied to the rapid diagnosis of these debilitating autoimmune diseases. The immobilisation of the La protein onto pSi films gave a protein receptor-decorated sensor matrix. A cascade of immunological reactions was then initiated to detect anti-La antibody on the functionalised pSi surface. In the presence of o-phenylenediamine (OPD), horseradish peroxidase (HRP)/H₂O₂ catalysed the formation of an oxidised radical species that accelerated pSi corrosion. pSi corrosion was detected as a blue-shift in the generated interference pattern, corresponding to a decrease in the effective optical thickness (EOT) of the pSi film. Compared to an ELISA, the pSi biosensor could detect the anti-La antibody at a similar concentration (500 – 125 ng/ml). Furthermore, we found that the experimental process can be significantly shortened resulting in detection of the anti-La antibody in 80 minutes compared to a minimum of 5 hours required for ELISA.

Keywords: biosensor, porous silicon, autoimmune, lupus, sjogren's

* Contact Author: jane0007@flinders.edu.au

1. INTRODUCTION

Traditionally, autoimmune disorders are detected by an enzyme-linked immunosorbent assay (ELISA). ELISAs are typically performed in polystyrene plates containing multiple wells, usually in a 96-well format, which are specifically designed for this purpose. While the ELISA is highly selective and sensitive method, the assay is time consuming and the throughput of this method is constrained by the dimensions the format of the multiwell plate. Newly developed biosensors based on pSi have been shown to be highly sensitive and specific, while also being compatible with high throughput formats including microarrays^[1]. The beneficial performance factors can be ascribed to pSi's optical and electronic properties and its large surface area. pSi biosensors have been used for the detection of a wide range of analytes (such as proteins, nucleic acids and living cells) by monitoring changes in optical and electrochemical signals on the substrate surface in response to the binding of target analytes^[2-6]. The sensing mechanisms of biosensors usually take advantage of naturally occurring reactions/interactions such as the interaction between an antibody and its antigen or the binding of complementary nucleic acids^[7].

Furthermore, readily available surface chemistry can be employed to functionalise pSi with bioelements. For example, pSi can be oxidised to obtain a surface with a high density of hydroxyl groups^[1, 8]. These surfaces can then be easily modified with alkoxysilanes to increase the stability of the pSi in solution and to generate a surface that is reactive towards biomolecular receptors.

Our research group recently discovered that horseradish (HRP)-catalysed oxidation of o-phenylenediamine (OPD) gave rise to an oxidised OPD species that accelerated the rate of pSi corrosion in solution^[9]. Analysis of this effect was carried out using an interferometer, where fast Fourier transformation (FT) converts pSi's characteristic Fabry-Perot fringe pattern into an effective optical thickness allowing real-time monitoring of surface events. This formed the basis of the biosensor's optical readout signal.

Auto-immune disorders affect a large fraction of the population and there is hence a significant need for fast and sensitive diagnostics methods for these debilitating diseases^[10]. Of particular interest to our group is the diagnosis of two auto-immune disorders, systemic lupus erythematosus (SLE) and Sjogren's Syndrome (SS). In SLE, auto-immune antibodies attack the host's tissue, causing inflammation, damage and pain in joints, kidneys, lungs, heart, blood vessels, the brain, the nervous system and skin^[11]. In SS, autoantibodies and immune system cells, called lymphocytes, attack the exocrine glands that produce tears, saliva and sweat, ultimately destroying the glandular tissue^[12]. While the causes of SLE and SS are unknown, an immunological relationship between the two diseases has been identified. It has been found that 15-25% of SLE sufferers and 50-90% of SS sufferers develop antibodies specific to a protein called La^[13, 14]. The La protein is found in all eukaryotic cells and associates with the 3' termini of newly synthesised small RNA's^[15]. The protein acts to stabilise the RNA and protect the 3' end from degradation due to endonucleases, allowing nuclear retention of RNA. Autoimmune antibodies against the La protein (anti-La antibody) are thought to prevent the La protein's physiological function. Therefore, detection of these antibodies is used as a diagnostic tool for these diseases^[16].

The goal of this work was to devise a pSi biosensor capable of the detection of anti-La antibodies by using the same optical transduction mechanism described above. Our basic approach involved the immobilisation of the La protein on the surface of pSi followed by introduction of the anti-La antibody, followed by the HRP-conjugated detection antibody. Enzymatic conversion of the substrate and subsequent pSi degradation then resulted in a measurable change in the reflective interference of the material (Figure 1).

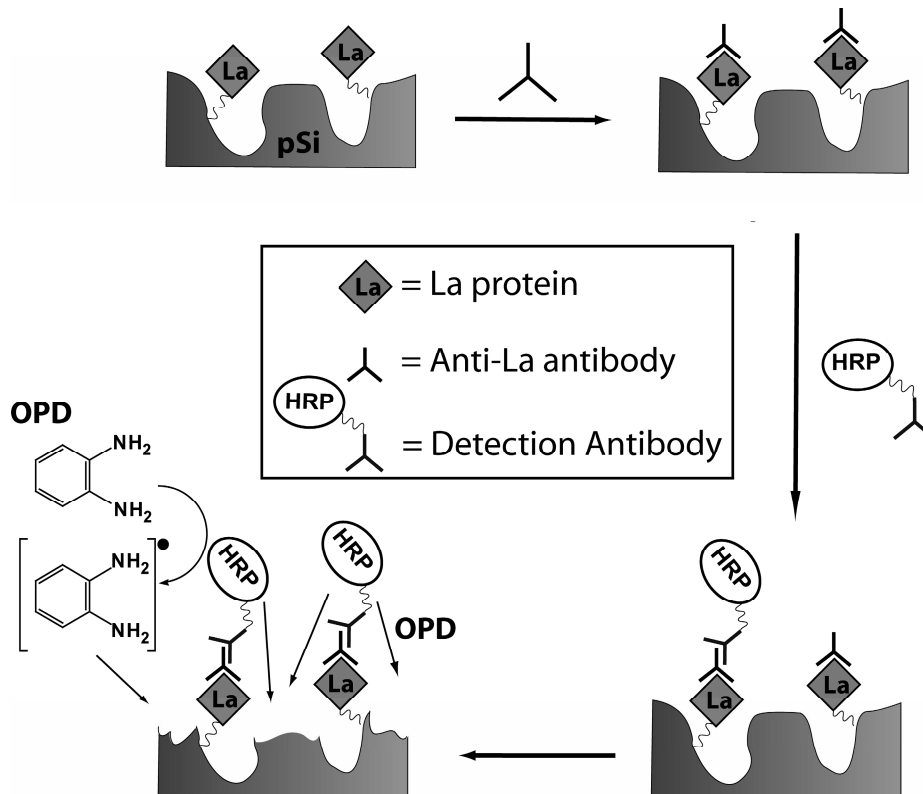


Figure 1: Schematic of the biosensor for anti-La antibodies based on enzyme catalysed pore corrosion of pSi.

2. EXPERIMENTAL

2.1 pSi formation.

Porous silicon films were produced by anodising highly doped p-type silicon (boron doped, 0.0005 - 0.001 Ω .cm resistivity, (100) orientation, Virginia Semiconductor Inc.) in a 3:1 mixture of 49% hydrofluoric acid (HF) and ethanol. Samples were etched at a current density of 450mA cm⁻² for 10 seconds.

2.2 Characterisation of pSi morphology.

Cross sectional analysis was performed by scanning electron microscopy (SEM) to ascertain the thickness of the pSi film. SEM was performed on a Phillips XL30 field emission scanning electron microscope with an acceleration voltage of 10kV and a capture angle of 90 and 45 degrees relative to the surface. Atomic force microscopy (AFM) was performed on the samples to reveal the surface morphology. AFM images of pSi were acquired on a Nanoscope IV Multimode microscope (Veeco Corp.) operating in tapping mode using silicon tips (FESP, Digital instruments) with a resonance frequency of 50-70 kHz. Image processing was done using Nanoscope v5.12 software.

2.3 pSi Chemical Modification of pSi.

Freshly etched samples were exposed to ozone (3.2g/hr) for 10 minutes to oxidise the surface. The oxidised pSi samples were silanised in 50mM 3-isocyanatopropyl triethoxysilane (Fluka) in toluene for 5 minutes at 25°C, washed extensively with toluene, dried with nitrogen and stored under vacuum.

2.4 Immobilisation of La protein.

The silanised samples were exposed to 1ml of 2 μ g/ml GST-LaA (Glutathione S-transferase fusion protein containing the 'A' subunit of the La protein) in phosphate buffered saline (PBS) (pH 7.4) and stirred on an orbital shaker for 2 hours. The sample was then washed with 3 x 1ml 0.5% Tween 20®, followed by 3 x 1ml PBS, before being exposed to 1ml of 1mM diethanoldiamine hydrochloride to quench any unreacted isocyanate groups. The sample was then rinsed with 3 x 1ml PBS and stored on ice prior to the sensing experiment.

2.5 Surface analysis of pSi.

The chemistry of the modified pSi surface was analysed using transmission mode infrared spectroscopy (IR) using a Nicolet Avatar 370MCT from Thermo Electron Corporation. Spectra were recorded and analysed using OMNIC version 7.0 software. Spectra were obtained in the range of 650-4000 cm^{-1} at a resolution of 1 cm^{-1} . All spectra were blanked using an un-etched silicon wafer of the same type.

2.6 Interferometric reflectance spectroscopy.

Figure 2 shows a schematic representation of the interferometric reflectance spectroscopy (IRS) (Ocean Optics, S2000) setup that was used to measure changes in EOT of the pSi layer. Freshly etched, oxidised and silanised pSi samples were placed into a custom built Plexi-glass flow cell (1.77 cm^2 diameter, 1mm thickness) and incubated in PBS for 15 minutes while monitoring the EOT.

2.7 Detection of anti-La antibodies.

Mouse anti-La antibody in a 50 μ g/ml bovine serum albumin (BSA) PBS solution was introduced to the sample for 20 minutes using the above mentioned flow cell. 0.5% (v/v) Tween® 20 in PBS was then flushed through the cell followed by PBS. The samples were incubated in PBS for 6 minutes before a sheep anti-mouse IgG conjugated to HRP (1:500) in a 50 μ g/ml BSA/PBS solution was injected and incubated over the pSi surface for 30 minutes. The sample was then washed as before with 0.5% (v/v) Tween® 20 and PBS. OPD (Sigma) (4mg/ml) in urea buffer was introduced and the change in the EOT slope was calculated. The flow cell was blocked for 12 hours with 2.5% BSA in PBS prior to each sensing experiment. All antibody solutions were prepared in 50 μ g/ml of BSA in PBS. For the negative controls, a random mouse IgG was used instead of anti-La and the protein GST was used in place of La.

2.8 ELISA Procedure.

A 96-well polystyrene plate was coated with 2 μ g/ml La protein in carbonate-bicarbonate buffer (pH 9.6) (100 μ l/well) and the other half with 2 μ g/ml of the control protein GST (100 μ l/well) in carbonate-bicarbonate buffer, covered with parafilm to prevent evaporation and incubated at 4 °C for 12 h. The plate was then washed three times with 0.05% (v/v) Tween® 20 in PBS (400 μ l/well) before being blocked with 2.5% (w/v) BSA in PBS (250 μ l/well) and incubated at 37 °C for 1 hour. The plate was washed as before with 0.05% (v/v) Tween® 20 in PBS. Anti-La antibody was serially diluted and added in duplicate to the plate (100 μ l/well) which was then incubated at 37 °C for 1 hour before being subjected to six washes with 0.05% Tween® 20. Anti-mouse IgG HRP conjugate (1:500, 100 μ l/well) was then added to each well and the plate incubated at 37 °C for 1 hour. The plate was then washed four times with Tween® 20 solution. The substrate OPD (100 μ l/well) was introduced to each well, covered with aluminium foil and allowed to develop. The plate was then read at 450nm (using a plate reader (Dynatech MR 600) at 10 and 30 minutes after addition of the substrate.

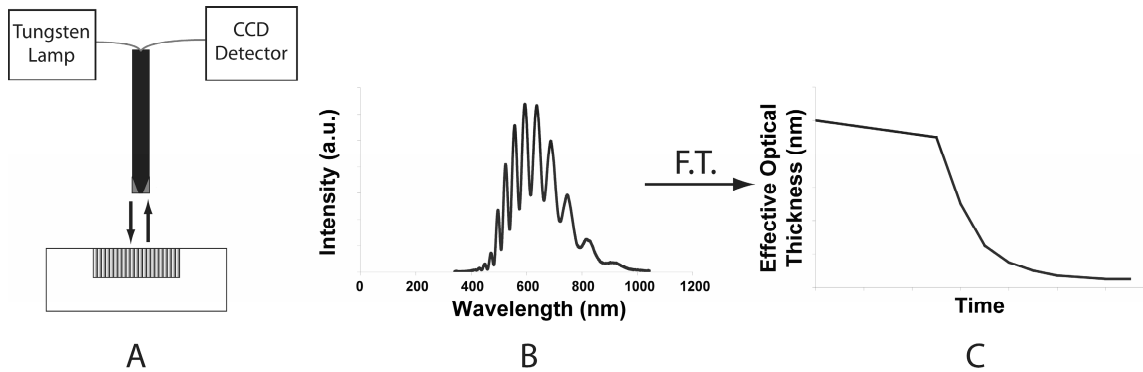


Figure 2: Interferometric Reflectance Spectroscopy. (A) White light produced by a tungsten light source is delivered through a bifurcated fiber optics cable and through a collimating lens impinging on the pSi layer at a 90° angle. The light is reflected back and enters into the detector fiber optics cable which delivers the light to the CCD spectrometer (Ocean Optics). (B) Due to constructive and destructive interferences, a Fabry-Perot fringe pattern is produced according to the equation $2nd = m\lambda$, where n = refractive index, d = layer thickness, m = fringe order, λ = wavelength. (C) Fourier transformation of the fringe pattern affords the effective optical thickness ($2nd$) which is tracked over time.

3. RESULTS & DISCUSSION

3.1 Pore Morphology

The etching conditions employed here gave macroporous silicon with a pore size of 60nm as determined by AFM (Figure 3A). This pore size was large enough to allow protein diffusion into the pores which was an essential requirement for this study. The SEM image in Figure 2B shows that the porous layer was $2.4 \mu\text{m}$ in thickness (Figure 3B). Pores were straight and showed little branching.

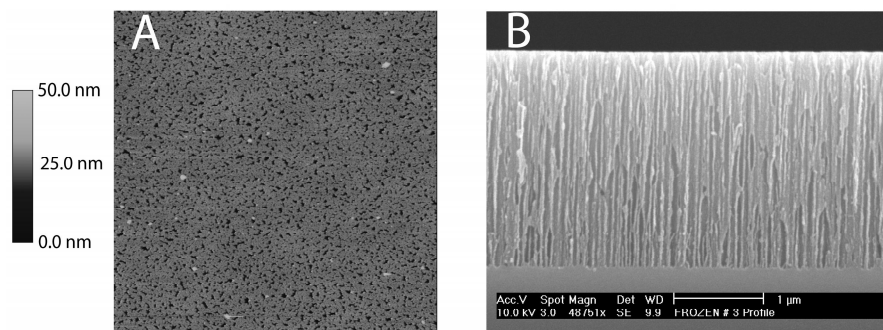


Figure 3: (A) AFM tapping mode height image of pSi, $5 \times 5 \mu\text{m}^2$. (B) Cross-sectional SEM micrograph of pSi layer on silicon.

3.2 pSi Functionalisation

Functionalisation of the pSi surface by oxidation and silanisation was carried out in order to protect the surface from degradation on exposure to the aqueous sensing medium and to provide an anchor point for protein immobilisation. The pSi functionalisation route employed here is shown in Figure 4.

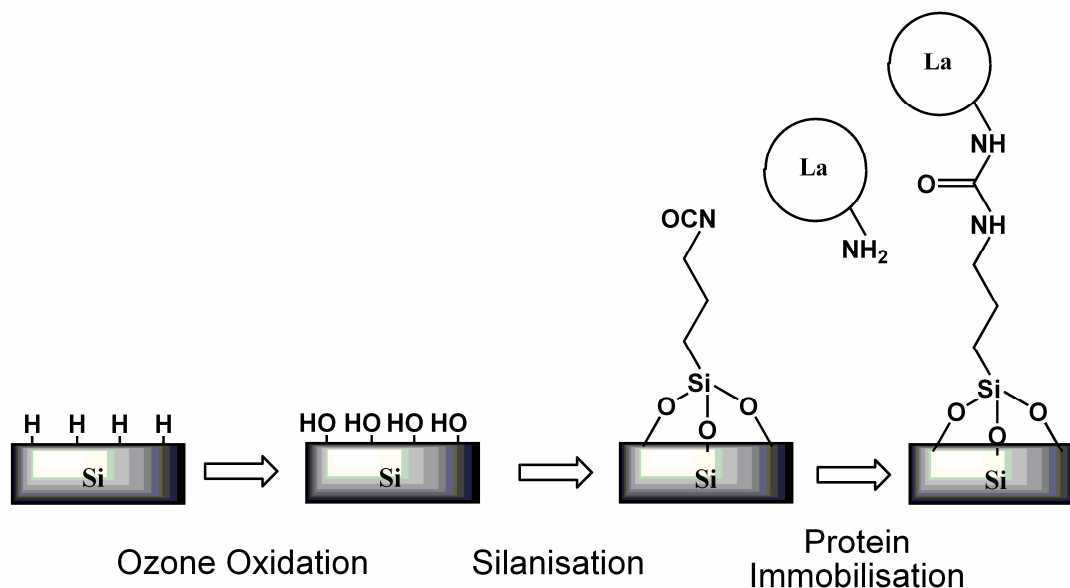


Figure 4: pSi functionalisation process. Freshly etched pSi was oxidised by exposure to ozone. Attachment of a silane linker, 3-isocyanatopropyl triethoxysilane, was then carried out. The La protein was then immobilised.

Figure 5 shows the resulting transmission IR spectra after each functionalisation step. The freshly etched pSi surface gave peaks at 900 cm^{-1} (SiH_2 scissor) and 2100 cm^{-1} denoting Si-H stretching vibrations in $\text{Si}_2\text{H-SiH}$ or $\text{Si}_3\text{-SiH}$. Upon oxidation the Si-H peaks completely disappear, replaced with a strong SiO peak in the region of 1100 cm^{-1} (SiO stretching in O-Si-O). This change in the spectra clearly shows that the ozone oxidation process has been successful, converting the surface to SiO_2 and SiOH. After silanisation with the isocyanato alkoxy silane, a peak at 2300 cm^{-1} appeared that was attributed to the N=C=O stretching vibration. The peaks over the range of $2850 - 3000\text{ cm}^{-1}$ are indicative of CH_2 groups. While the peaks at $\sim 1550\text{ cm}^{-1}$ (N-H bending) and 3640 cm^{-1} (N-H stretching) represent the presence of amine groups and the peak at 1702 cm^{-1} represents a carbonyl group (C=O stretching), indicating that some of the silane molecules have cross-linked. This phenomenon is possibly due to a reaction between the isocyanate groups and residual water in the solvent or due to water vapour in the air during sample handling and characterisation, leading to the formation of carbamates, which then dissociates into carbon dioxide and an amine. The amine then reacts with neighbouring isocyanates leading to a urea cross-link^[17].

After immobilisation of the La protein, the peak at 2300 cm^{-1} disappeared, indicating that all of the isocyanate groups had reacted with the protein or had become cross-linked in contact with the aqueous medium. It was observed that immobilisation of the La protein led to a slight shift in the carbonyl peak to lower wavenumbers ($1680\text{-}1690\text{ cm}^{-1}$). This peak is indicative of C=O stretching in peptide bonds present in proteins. Additional analysis revealed the appearance of a peak in the region of 3720 cm^{-1} which was attributed to amide N-H stretching vibrations, providing further evidence for the presence of the La protein. The peak at 1550 cm^{-1} corresponding to the amine N-H bending vibration has broadened, also suggesting the presence of protein. IR analysis therefore provided evidence that each step of the immobilisation process for La protein was successful.

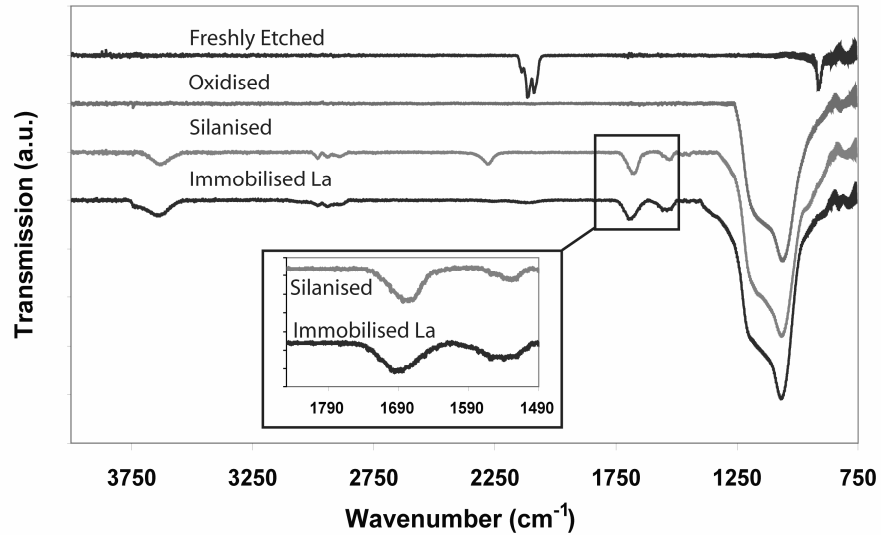


Figure 5: Transmission IR spectra taken on freshly prepared pSi, after ozone oxidation, silanisation and immobilisation of La protein.

The effect of surface functionalisation procedures on the stability of the pSi films was analysed in aqueous medium of physiological pH (7.4). The stability of the pSi film in aqueous medium is essential for the performance of this biosensor as rapid corrosion in the environment used for biosensing would result in poor performance of the biosensor and/or shorter biosensor life-span. Figure 6 shows the EOT of the functionalised pSi films over time. The EOT of the freshly prepared pSi (Figure 6A) decreased rapidly indicating a fast rate of pSi corrosion. This was expected because non-oxidised pSi films are susceptible to oxidative hydrolysis in aqueous medium^[1, 18]. After ozone oxidation (Figure 6B), the Si-H pSi surface was capped by Si-O species, which protected the surface from hydrolytic degradation and hence only a small decrease in EOT was observed on this surface. Further functionalisation of the pSi surface with the alkoxysilane (Figure 6C) afforded even greater stability to the pSi film because of the resulting siloxane film.

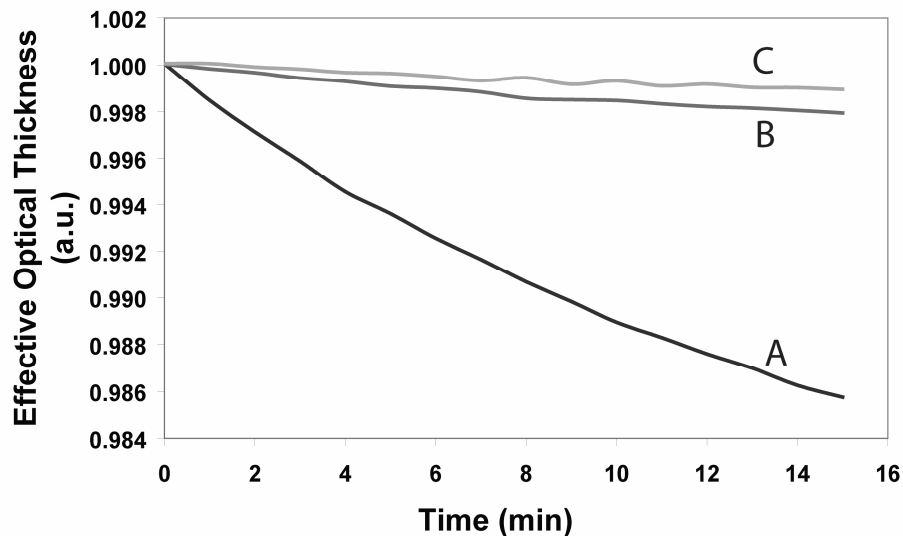


Figure 6: Degradation of functionalised pSi samples in PBS. (A) Freshly etched pSi, (B) ozone oxidised pSi, (C) silanised pSi.

3.3 Biosensing of Anti-La Antibodies

La protein functionalised pSi was exposed to the anti-La antibody, followed by a HRP conjugated anti-La detection antibody and finally to OPD. Figure 7 shows the detection of anti-La via HRP/H₂O₂ oxidation of OPD. Upon injection of OPD, the EOT sharply decreased, representing a blue shift in the Fabry-Perot fringe pattern and rapid corrosion of the pSi layer. Although the exact corrosion mechanism is unknown, we postulate that the oxidised OPD radical intermediate produced by HRP^[19, 20] (Figure 8) may enforce the oxidative hydrolysis of pSi into products such as silicic acid (Si(OH)₄) and silica (SiO₂). This hypothesis is also consistent with the observed levelling out of the rate of pSi degradation over time. Initial oxidation of OPD results in high concentrations of the intermediate species and a rapid decrease in EOT. However after ~30 minutes of HRP/H₂O₂-catalysed oxidation of OPD, the final stable oxidised product accumulates and the concentration of the intermediate decreases. This factor combined with the formation of un-reactive silica on the pore surface and the removal of the La protein from proximity to the pore walls due to corrosion effects, would contribute to the stabilisation of EOT slope.

Control experiments using a random mouse IgG in the place of anti-La (Figure 7) and the replacement of immobilised La with GST (not shown) resulted in no change to the EOT slope upon addition of OPD (Figure 7). This indicated that the sensor is specific to anti-La and that the degradation of pSi occurs in the presence of oxidised OPD.

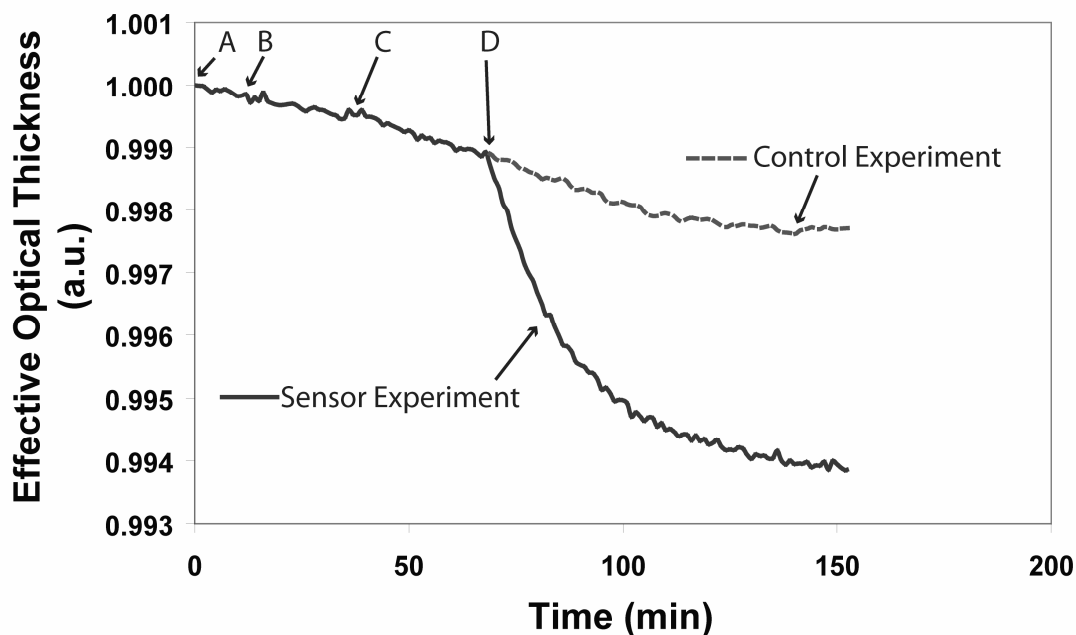
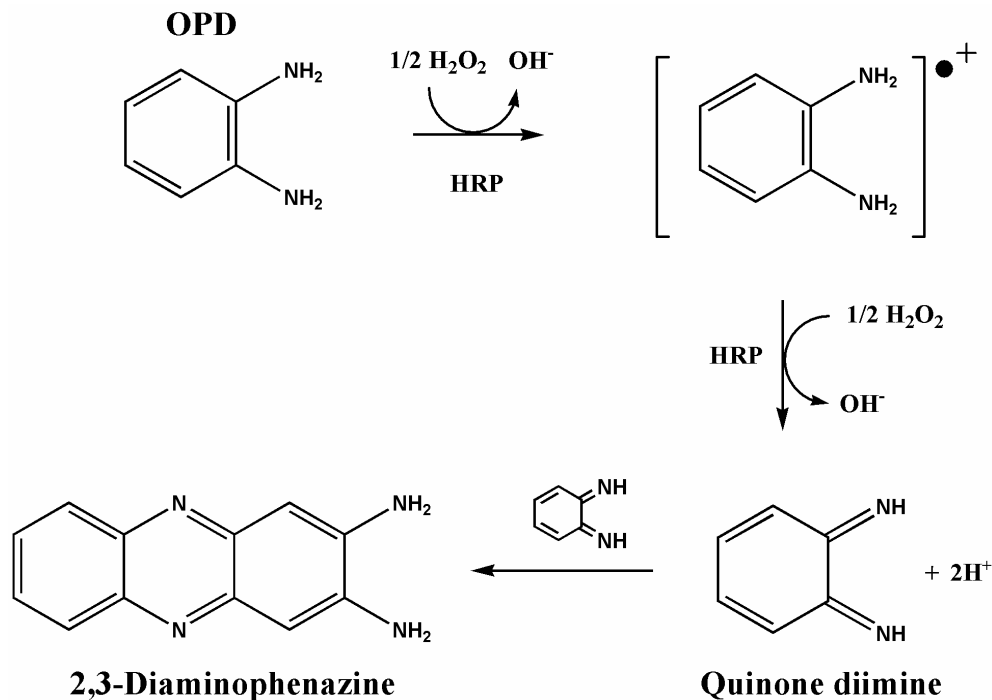


Figure 7: Changes in effective optical thickness of a La protein functionalised pSi surface upon incubation with anti-La antibodies. (A) Baseline in PBS was achieved, (B) addition of Anti-La antibody solution (200ng/ml), (C) addition of IgG-HRP (1:500) and (D) addition of OPD solution (4mg/ml). Sensor experiment is shown as a solid line, while the IgG control is shown as a dashed line.


 Figure 8: Oxidation pathway of OPD when catalysed by HRP/H₂O₂ ^[19, 20]

3.4 Comparison of ELISA and pSi Biosensor

To compare the effectiveness of the pSi biosensor to a standard ELISA, a series of concentrations were analysed by both techniques (Figure 9). ELISA experiments for the detection of anti-La revealed a linear relationship between absorbance and concentration, providing strong sensitivity down to antibody levels of ~30 ng/ml. The pSi sensor revealed a correlation between the signal strength (EOT detection slope) and the concentration of anti-La antibodies. Unlike in the ELISA the correlation was not linear.

The considerable optical signal achieved at an antibody concentration of 125ng/ml was encouraging as it indicates that the sensor has the ability to detect low concentrations of anti-La antibodies due to the signal amplification achieved by enzyme-catalysed pore corrosion. This result is promising, since typical anti-La antibody levels in serum of patients suffering from SLE or SS are generally in the range of mg to µg/ml, indicating that the pSi biosensor might have sufficient sensitivity to detect antibodies in clinical samples ^[21].

Further investigations into the effect of antibody concentration on the detection signal on the pSi biosensor are required before a comprehensive comparison between the accuracy of the two detection methods can be made.

Comparison between the two techniques showed a significant difference in the detection time. Whilst the ELISA technique required a minimum 5 hours of analysis time, the pSi sensor required only 80 minutes to detect the same anti-La antibody sample.

This results shows that the enzyme catalysed degradation of pSi is able to achieve faster detection and diagnosis of anti-La antibodies and possibly of other disease markers. The reduced detection period has significant practical implications such as reduced labour costs or higher sample throughput.

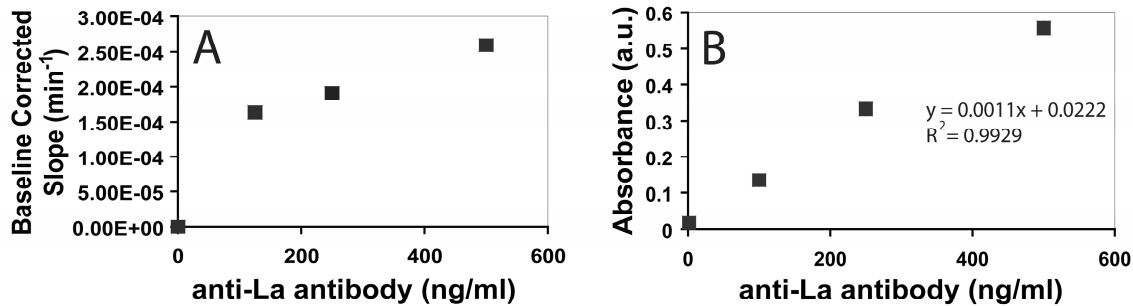


Figure 9: Calibration curve for (A) pSi sensor for anti-La concentrations, 125ng/ml – 1000ng/ml. (B) ELISA for anti-La concentrations, 100ng/ml – 500ng/ml.

CONCLUSION

In conclusion, a pSi film was used to detect the binding of antibodies to a covalently immobilised La protein capture probe, by means of enzyme-catalysed corrosion of the pSi. Corrosion of the pSi by degradation and oxidation gave rise to distinct changes in the EOT which amplified the initial binding event. Admittedly, the signal amplification observed herein is limited by the turnover rate of the enzyme and by the removal of catalytically active site on the surface due to corrosion. The approach described here is compatible with an array format (enabling high throughput detection), requires only inexpensive device components such a CCD spectrometer and a light source and is conducive to miniaturization. In comparison to a standard ELISA, detection time was significantly reduced. Our biosensor may therefore find practical applications as a new tool for the diagnosis of La related autoimmune diseases.

ACKNOWLEDGEMENTS

The authors gratefully acknowledge financial support from the Australian Research Council's Discovery Project scheme.

REFERENCES

1. Stewart, M.P., *Chemical and biological applications of porous silicon technology*. Advanced Materials, 2000. **12**(12): p. 859-869.
2. Mathew, F.P., *Porous silicon-based biosensor for pathogen detection*. Biosensors & Bioelectronics, 2005. **20**(8): p. 1656-1661.
3. Setzu, S., *Porous silicon-based potentiometric biosensor for triglycerides*. Physica Status Solidi A-Applications and Materials Science, 2007. **204**(5): p. 1434-1438.
4. Song, M.J., *Electrochemical biosensor array for liver diagnosis using silanization technique on nanoporous silicon electrode*. Journal of Bioscience and Bioengineering, 2007. **103**(1): p. 32-37.
5. Steinem, C., Janshoff, A., Lin, V.S., Voelcker, N.H., Ghadiri, M.R., *DNA hybridisation-enhanced porous silicon corrosion: mechanistic investigations and prospect for optical interferometric biosensing*. Tetrahedron, 2004. **60**: p. 11259-11267.
6. Alvarez, S.D., *Using a porous silicon photonic crystal for bacterial cell-based biosensing*. Physica Status Solidi A-Applications and Materials Science, 2007. **204**(5): p. 1439-1443.
7. Yamaguchi, R., *DNA hybridization detection by porous silicon-based DNA microarray in conjugation with infrared microspectroscopy*. Journal of Applied Physics, 2007. **102**(1).
8. Janshoff, A., *Macroporous p-type silicon Fabry-Perot layers. Fabrication, characterisation and applications in biosensing*. Journal of the American Chemical Society, 1998. **120**: p. 12108-12116.
9. Szili, E.J., *Unpublished PhD Thesis, in SoCPES*. Submitted 2007, Flinders University: Adelaide.

10. Trager, J., Ward., M.M., *Mortality and causes of death in systemic lupus erythematosus*. Current Opinion in Rheumatology, 2001. **13**: p. 345-351.
11. Lahita, R., G., *Systemic Lupus Erythematosus*. 4 ed. 2004: Academic Press. 1343.
12. Dauphin, S., *Understanding Sjogren's Syndrome*. 1993: Pixel Press. 244.
13. Wahren, M., Tengner, P., Pettersson, I., *Ro/SS-A and La/SS-B antibody level variation in patients with Sjogren's syndrome and systemic lupus erythematosus*. Journal of Autoimmunity, 1998. **11**: p. 29-38.
14. Tengner, P., Halse, A., Haga, H., *Detection of anti-Ro/SSA and anti-La/SSB autoantibody-producing cells in salivary glands from patients with Sjogren's syndrome*. Arthritis & Rheumatism, 1998. **12**(41): p. 2238-2248.
15. Wolin, S.L., *The LA protein*. Annual Review of Biochemistry, 2002. **71**: p. 375-403.
16. Pruijn, G.J.M., *The La (SS-B) antigen*, in *Manual of Biological Markers of Disease*, W.J.M. Van Venrooij, R. N., Editor. 1994, Kluwer Academic Publishers.
17. Clayden, J., Greeves, N., *Organic Chemistry*. 2001: Oxford University Press. 1508.
18. Allongue, P., *Etching of silicon in NaOH solutions: Electrochemical studies of n-Si(111) and n-Si(100) and the mechanism of the dissolution*. Journal of the Electrochemical Society, 1993. **140**(4): p. 1018-1026.
19. Claiborne, A., Fridovich, I., *Chemical and enzymatic intermediates in the peroxidation of o-dianisidine by horseradish peroxidase*. Biochemistry, 1979. **18**(11): p. 2324-2329.
20. Muginova, S.V., *Kinetics and pathways of oxidation of o-phenylenediamine, 3,3'-dimethoxybenzidine, and 3,3',5,5'-tetramethylbenzidine with hydrogen peroxide, catalyzed with horse radish peroxidase immobilized on various supports*. Russian Journal of Applied Chemistry, 1999. **72**(5): p. 840-846.
21. Gordon, T.P., *Estimation of amounts of anti-La(SS-B) antibody directed against immunodominant epitopes of the La(SS-B) autoantigen*. Clinical and Experimental Immunology, 1991. **85**(3): p. 402-406.